HHS Public Access

Author manuscript

Calcif Tissue Int. Author manuscript; available in PMC 2017 September 01.

Published in final edited form as:

Calcif Tissue Int. 2016 September ; 99(3): 289–301. doi:10.1007/s00223-016-0149-z.

Changes in the Fracture Resistance of Bone with the Progression of Type 2 Diabetes in the ZDSD Rat

Amy Creecy[1,2,3], **Sasidhar Uppuganti**[1,3,4], **Alyssa R. Merkel**[3], **Dianne O'Neal**[5], **Alexander J. Makowski**[1,2,3], **Mathilde Granke**[3,4], **Paul Voziyan**[6], and **Jeffry S. Nyman**[1,2,3,4]

[1]Department of Veterans Affairs, Tennessee Valley Healthcare System, Nashville, TN 37212

[2]Department of Biomedical Engineering, Vanderbilt University, Nashville, TN 37232

[3]Center for Bone Biology, Vanderbilt University Medical Center, Nashville, TN 37232

[4]Department of Orthopaedic Surgery & Rehabilitation, Vanderbilt University Medical Center, Nashville, TN 37232

[5]School of Medicine, Meharry Medical College, Nashville, TN 37208

[6]Department of Medicine, Vanderbilt University Medical Center, Nashville, TN 37232

Abstract

Individuals with type 2 diabetes (T2D) have a higher fracture risk compared to non-diabetics, even though their areal bone mineral density is normal to high. Identifying the mechanisms whereby diabetes lower fracture resistance requires well-characterized rodent models of diabetic bone disease. Toward that end, we hypothesized that the bone toughness, more so than bone strength, decreases with the duration of diabetes in ZDSD rats. Bones were harvested from male CD(SD) control rats and male ZDSD rats at 16-wks (before the onset of hyperglycemia), at 22-wks (5–6 wks of hyperglycemia), and at 29-wks (12–13 wks of hyperglycemia). There were at least 12 rats per strain per age group. At 16-wks, there was no difference in either body weight or glucose levels between the 2 rat groups. Within 2 weeks of switching all rats to a diet with 48% of kcal from fat, only the ZDSD rats developed hyperglycemia (>250 mg/dl). They also began to lose body weight at 21-wks. CD(SD) rats remained normoglycemic (<110 mg/dl) on the high fat diet and became obese (>600 g). From micro-computed tomography (μCT) analysis of a lumbar vertebra and distal femur, trabecular bone volume did not vary with age among the non-diabetic rats but was lower at 29-wks than at 16-wks or at 22-wks for the diabetic rats. Consistent with that finding, μCT-derived intra-cortical porosity (femur diaphysis) was higher for ZDSD following ~12 wks of hyperglycemia than for age-matched CD(SD) rats. Despite an age-related increase in mineralization in both rat strains (μCT and Raman spectroscopy), material strength of cortical bone (from three-point bending testing) increased with age only in the non-diabetic CD(SD) rats. Moreover, two other material properties, toughness (radius) and fracture toughness (femur), significantly decreased with the duration of T2D in ZDSD rats. This was accompanied by the increase in the levels of the pentosidine (femur). However, pentosidine was not significantly higher in diabetic than in non-diabetic bone at any time point. The ZDSD rat, which has normal leptin

Contact: Jeffry S. Nyman, 1215 21st Ave. S., South Tower, Suite 4200, Nashville, TN 37232, jeffry.s.nyman@vanderbilt.edu office: (615) 936-6296 fax: (615) 936-0117.

signaling and becomes diabetic after skeletal maturity, provides a pre-clinical model of diabetic bone disease, but a decrease in body weight during prolonged diabetes and certain strain-related differences before the onset of hyperglycemia should be taken into consideration when interpreting diabetes-related differences.

Keywords

type 2 diabetes; bone quality; advanced glycation end-products; porosity; Raman spectroscopy; micro-computed tomography; mechanical testing; pentosidine

1. Introduction

There is a growing population of individuals with diabetes who are prone to fractures [1, 2]. A meta-analysis of epidemiological studies estimated that individuals with type 2 diabetes (T2D) are approximately two times more likely to suffer a hip fracture than non-diabetics of the same age and gender [3]. Furthermore, greater fracture risk in diabetic patients is disproportionate to differences in areal bone mineral density (aBMD) between diabetic and age-matched healthy individuals [4, 5]; and the incidence of hip fracture is higher in long-term compared with short-term diabetes [3, 6]. These observations stress the need for i) understanding how duration of diabetes affects bone beyond aBMD and ii) developing treatment strategies that improve the inherent quality of the bone matrix beyond simply increasing the amount of bone.

The clinical observation that the age-adjusted fracture risk for a given femoral neck aBMD is higher among adults with T2D than among the non-diabetic adults [7] suggests that T2D lowers fracture resistance through deleterious effects on the material properties of bone. Clinical studies using peripheral computed tomography (HR-pQCT), an imaging technique capable of resolving cortical and trabecular thickness at the distal sites, do not report worsening of cortical structure or trabecular architecture in elderly women with T2D compared to age-matched non-diabetics [8, 9]. However, there is evidence of increased intra-cortical porosity in some diabetic cohorts [8, 10], especially if the T2D patient had suffered a fracture [11]. Likewise, T2D post-menopausal women with a fracture had thinner cortices at the femoral neck compared to those without fractures [12]. Worsening of bone material properties in diabetes would explain the paradox that aBMD is higher among diabetics compared to non-diabetics, even though diabetes elevates fracture risk [13].

Unlike material strength (independent of structure) that assesses the ability of a bone to resist permanent deformation, toughness assesses the ability of bone to dissipate energy during failure. For cortical bone, deformation after yielding primarily dictates toughness and primarily depends on the collagen phase. Moreover, there is an association between the age-related decrease in bone toughness or post-yield toughness and the increase in non-enzymatic, glycation-mediated collagen crosslinks (NEGs) [14]. One of these NEGs, pentosidine (PE), is the standard biomarker for advanced glycation end-products (AGEs) in bone [15]. Mechanistically, AGE accumulation in the bone matrix is thought to impede collagen fibril deformation, thus reducing energy dissipation and subsequently the fracture resistance of bone [16]. Other major AGE crosslinks such as glucosepane are not yet readily

measurable in bone [17]. Nonetheless, a diabetic increase in overall bone PE has been directly observed in one study to date [18]. In addition to hyperglycemia, oxidative stress enhances non-enzymatic glycation of collagen [19] as the AGE formation often requires an oxidative step. Thus, diabetic bone disease could be more a problem of bone brittleness and less a problem of low bone strength.

The prominent phenotype of most diabetic rat models is structural weakness when compared to age- and gender-matched non-diabetic controls. This has been observed in both cortical and trabecular bone [20, 21] with diabetic rats having lower peak force for both the bending of the femur mid-shaft [21, 22] and the compression of lumbar vertebrae [22, 23]. This difference accompanied lower volumetric BMD for both cortical and trabecular bone [20–22]. In the Zucker Diabetic Fatty (ZDF) model, the cross-sectional moment of inertia, cortical thickness, and cortical volumetric bone mineral density are all lower in the diabetic than in the non-diabetic rats [21, 22]. However, the differences in bone material properties are not always reproducible and appear to depend on the duration and onset of diabetes [24, 25].

To advance clinically relevant diagnostic and therapeutic tools, there is a need for pre-clinical models of diabetes in which the fracture resistance of bone decreases with disease progression. Therefore, a thorough assessment of bone changes in rodent models of type 2 diabetes is required [25]. Including analysis of bones from rats before diabetic onset for the first time, we characterized how the fracture resistance of bone decreases as diabetes progresses in a diet-induced, adult-onset rat model of T2D. In particular, mechanical properties not dependent on aBMD or bone structure were measured in addition to whole-bone strength.

2. Materials and Methods

2.1. Study Design

Twenty-six male CD(SD) rats and 38 male Zucker Diabetic Sprague-Dawley (ZDSD) rats between 6 weeks and 8 weeks of age were purchased from Charles River (Wilmington, MA) and PreClinOmics (Indianapolis, IN), respectively. As one of the parental strains of the ZDSD rat, the CD(SD) rat serves as the non-diabetic control [20, 23, 26, 27]. Under the advisement of PreClinOmics, all rats were switched from standard chow (Purina 5008, LabDiet, St. Louis, MO) to a diet in which 47.7% kcal came from fat (5SCA, TestDiet, Richmond, IN) *ad libitum* at 16 weeks of age. Rats were switched back to 5008 after 6−7 weeks. Female ZDSD rats are less resistant to diabetes with one-third to one-half experiencing hyperglycemia at variable ages on a high fat diet (HFD) such as 5SCA [20]. Non-fasting blood glucose levels were periodically measured using a glucometer (TRUEresult®, Nipro Diagnostics, Inc., Fort Lauderdale, FL). Four ZDSD rats died or were killed early because they lost 20% of their body weight. Two animals were excluded from the study because they either did not develop diabetes or were only hyperglycemic (>250 mg/dL) for 1 week. As such, bones were harvested from 12 CD(SD) and 14 ZDSD rats at 22 weeks of age and from 14 CD(SD) and 18 ZDSD rats at 29 weeks of age. Fourteen young male CD(SD) and twelve age-matched male ZDSD rats were also purchased and euthanized at 16-wks without being fed the HFD. None of these rats were hyperglycemic. We used

procedures including the method of euthanasia that were approved by the local Institutional Animal Care and Use Committee, which follows the *Guide for the Care and Use of Laboratory Animals* (8^{th} edition, The National Academies Press, Washington, DC).

2.2. Micro-computed tomography analysis (μCT)

Bones were first imaged using a high-resolution μCT scanner (μCT50, Scanco Medical, Brüttisellen, Switzerland) at isotropic voxel sizes of 10 μm (intact long bones and L6 vertebra), and 12 μm (notched femur). The regions of interests (ROIs) were: i) a 4 mm section in the central mid-shaft of an intact femur (right), ii) a 5 mm section of the distal femur metaphysis (right), iii) a 4 mm region centered around a micro-notch generated in the posterior side of the contralateral femur (left), iv) a 1.86 mm section centered at the point of curvature within the radius diaphysis, and v) the L6 VB (from cranial to caudal end-plates). Using weekly calibration scans of a hydroxyapatite (HA) phantom and a beam hardening correction, linear X-ray attenuation coefficients were converted to volumetric tissue mineral density (TMD).

Post reconstruction, the manufacturer's contouring and evaluation scripts provided standard structural (e.g., Ct.Th, Ct.Ar, I_{min}, C_{min}), compositional (e.g., Ct.TMD, Tb.TMD), and morphological parameters (e.g., BV/TV, Tb.N, Tb.Th., Conn.D) of bone following published guidelines [28]. As described in our previous study [29], a global threshold with noise filtering was selected for each region to segment bone from soft tissue and air or pores from bone.

2.3. Biomechanical analysis

2.3.1 Quasi-static flexural tests of femur and radius—With the anterior side of the diaphysis facing down, each hydrated bone was monotonically loaded in three-point (3pt) bending at 3.0 mm/min until failure (DynaMight 8841, Instron, Norwood, MA). The span (L) of the lower supports was 14 mm for the radius and between 15 mm and 17 mm for the femur (span ≈ 5×anterior-posterior width). The structure-dependent properties included rigidity (stiffness × L^3 / 12), peak moment (M_p), and work-to-failure (W_f) adjusting for the span. Then, using the μCT-derived structural parameters, we estimated the modulus (rigidity / I_{min} / 4), material strength or peak bending stress (M_p × C_{min} / I_{min} / 4), and toughness (3 × W_f / Ct.Ar / L) as previously described for the analysis of force vs. displacement data from a flexural test [29, 30]. Post-yield displacement (PY_{disp}) was measured as displacement between the yield point and the displacement at fracture.

2.3.3. Fracture toughness testing of notched femur—After generating a micro-notch at the mid-point of the diaphysis on the posterior side [29], the contra-lateral femurs were also monotonically loaded to failure in 3pt bending but at 0.06 mm/min and with the posterior side facing down in order to propagate a crack. Using the previously published equations presented in [31], the fracture toughness was determined as the critical stress intensity (K_c) occurring at the initial micro-notch under the peak force endured by the bone. Cracking toughness (i.e. energy to propagate the crack) was measured by the span-adjusted W_f divided by the Ct.Ar.

2.4. Compositional analyses

2.4.1. Raman spectroscopy (RS)—Following our previously described methods for Raman analysis of intact mouse femurs [32, 33], each rat femur (right) was mounted with the anterior side facing up under a 50× objective (NA = 0.75) of a confocal Raman microscope (InVia, Renishaw, Hoffman Estates, IL) equipped with a 785 nm laser diode source (Innovative Photonic Solutions, Monmouth Junction, NJ). After blotting the wet surface with a Kimwipe, the periosteal surface was brought into focus under the bright field. At 3 sites along the mid-shaft (Fig. 1), spectra were collected with 7 accumulations of 12 s exposures of 35 mW laser power. Following cosmic spike removal and subtraction of background fluorescence [33], the spectra provided compositional properties as follows: the mineral-to-matrix ratio, type B carbonate substitution, and crystallinity (Fig. 1). The average of the 3 sites per bone was used in the statistical analysis.

2.4.2. High performance liquid chromatography (HPLC)—HPLC analysis was performed on a 4 mm cross-section of the left femur mid-shaft after biomechanical testing. Bone segments were demineralized in 20% ethylenediaminetetraacetic acid (EDTA) at 4 °C. The segments were hydrolyzed in 6 N HCl with 4.5 mM alpha-amino-N-butyric acid (α-ABA) for ~20 hours. To determine collagen content, 500 μL of ethanol, triethyleneamine and water (2:1:2) were first added to ~1 mg of each filtered sample as well as to standards consisting of hydroxyproline, proline and α-ABA. They were subsequently derivatized with ethanol, water, phenylisothiocyanate (PITC), and triethyleneamine (7:1:1:1) and re-suspended in a diluent buffer of 0.071% disodium phosphate (NaH_2PO_4) in 5% acetonitrile [34]. Samples and standards were injected into a column for hydrolysate amino acid analysis (Waters PicoTag®, Milford, MA). And the amino acids were eluted using 1.9% sodium acetate plus 0.05% acetonitrile and 60% acetonitrile as the mobile phase (Beckman Coulter System Gold 126, Brea, CA). The chromatogram was generated using a UV detector (Beckman Coulter 168 Detector, Brea, CA). Collagen content was determined from the measurement of hydroxyproline. Since the hydroxyproline was 2 times higher than the expected value for 8 of the 84 samples, a correction was applied based on the regression between collagen mass and wet mass.

To determine crosslink concentrations, another portion of the hydrolyzed bone sample was re-suspended in 0.25 μg/mL of pyridoxine (PYR) in HPLC-grade water. The samples were mixed (1:1) with dilution buffer, which consisted of 10% HPLC-grade acetonitrile and 0.5% heptafluorobutryic (HFBA) as the ion-pairing agent. Samples were injected along with standards consisting of PYR and varying concentrations of pyridinoline (PYD), deoxypyridinoline (DPD) and pentosidine (PE) into a silica-based, reversed-phase C18 column (Waters Spherisorb® 5μm ODS2, Milford, MA). Crosslinks were separated with two mobile phases of 0.22% HFBA and 100% acetonitrile. A programmable fluorescence detector (Waters 2475 Multi λ Fluorescence Detector) was used to generate chromatograms. Moles of each crosslink per sample were divided by the corresponding moles of collagen.

2.5. Statistical analysis

All statistical analyses were done using GraphPad Prism (v6.0a, GraphPad Software, Inc., La Jolla, CA). Because the majority of the outcome measures either did not pass the

Shapiro-Wilk normality test for at least one experimental group or the variance was significantly different among the 6 experimental groups (Brown-Forsythe Test), the Kruskal-Wallis test was used to determine whether each property differed among the experimental groups. When group means were not the same, three different multiple pair-wise comparisons were done: i) 16-wk vs. 22-wk, 16-wks vs. 29-wks, and 22-wks vs. 29-wks within CD(SD), ii) 16-wks vs. 22-wks, 16-wks vs. 29-wks, and 22-wks vs. 29-wks within ZDSD, and iii) CD(SD) vs. ZDSD within each age group (16-wks, 22-wks, and 29-wks). In each of these post-hoc tests of 3 comparisons, the non-parametric Dunn's test provided the adjusted p-value for a family-wise significance level of 0.05. Differences in body weight and glucose between the rat strains were determined using Mann-Whitney tests at each time point.

3. Results

3.4. Changes in weight and in glucose levels with the progression of diabetes

Other than one ZDSD rat that was diabetic (≥250 mg/dL) at baseline, the ZDSD rats became diabetic within 2 weeks of switching from standard chow to the 5SCA HFD (Fig. 2a). The control CD(SD) rats remained normoglycemic (Fig. 2a) and became obese on the HFD (Fig. 2b). The ZDSD rats on the HFD actually lost weight as the duration of T2D increased (Fig. 2b).

3.5. Loss of trabecular bone with progression of diabetes

In the distal femur metaphysis (DFM) and L6 VB, the trabecular bone volume fraction did not change in CD(SD) rats between 16-wks and 29-wks of age, whereas it declined significantly in diabetic ZDSD rats (Table 1). During the 12–13 weeks of diabetes that the ZDSD rats experienced, the trabeculae became thinner, whereas Tb.Th increased in non-diabetic controls over the same time period, namely in the VB (Table 1). Also, there were fewer trabeculae at 29-wks than at 16-wks for only the ZDSD rats. Differences in connectivity density (Conn.D) between the rat strain were not significant, regardless of age. The tissue mineral density of trabeculae (Tb.TMD) increased with age (DFM and VB) in both diabetic and control rats. However, the rate increase was lower among the ZDSD rats such that Tb.TMD was significantly lower for the diabetic than for the non-diabetic rats at 29-wks.

3.6. Strain-related differences in cortical structure but diabetes-related differences in microstructure

For both long bones, we found structural differences in the cortex of the mid-shaft between CD(SD) and ZDSD rats that were independent of diabetes. The average moment of inertia (I_{min}) of the diaphysis, the periosteal perimeter (Ps.Pm), and the length of the long bones were lower in the ZDSD than in CD(SD) rats at all age groups (Table 2). Regardless of rat strain, I_{min}, cross-sectional area of cortical bone (Ct.Ar), and cortical thickness (Ct.Th) of each mid-shaft were lower at 16-wks than at 22-wks and 29-wks. In effect, T2D did not affect normal age-related increase in structure of either long bone between 16-wks and 22-wks. This is also evident in total cross-sectional area (Tt.Ar) and Ps.Pm, which were higher for the older ZDSD rats than for 16-wk rats (Table 2).

Unlike the structural parameters, there were no strain-related differences in intra-cortical porosity (Ct.Po) at 16-wks or 22-wks of age (Fig. 3). However, there was a diabetes-related increase in Ct.Po of the femur mid-shaft such that Ct.Po and pore number was higher in the diabetic rats than in control rats at 29-wks of age (Fig. 3).

3.7. Similar age-related changes in biomechanical properties of non-diabetic and diabetic bone

Given the age-related increase in I_{min}, whole-bone strength and rigidity of both the radius and femur were higher at 29-wks than at 16-wks for both strains (Table 2). Before the change in diet, the radius was stronger for the CD(SD) than for the ZDSD rats, but no strain-related difference in peak moment (M_p) existed for the femur. Post-yield displacement (PY_{disp}) of the femur did not vary among the groups, while PY_{disp} of the radius decreased with age for both rats with it being less for the diabetic ZDSD rats, though not statistically significant.

3.8. Diabetes-related changes in the estimated material properties

The material strength or peak bending stress of cortical bone significantly increased from 16 to 29-wks of age in the CD(SD) rats, whereas it did not significantly vary with age in the diabetic ZDSD rats (Fig. 4a). Interestingly, Ct.TMD, a determinant of material strength, increased with age for both rat strains (Table 2). Compared to 16-wks, toughness (radius only) was lower at 22-wks and at 29-wks in only the diabetic rats (Fig. 4b). Unlike bending strength, there were no differences in toughness between the strains at 16-wks of age, but toughness (radius only) was significantly lower for the diabetic bone than non-diabetic bone at 29-wks. When a crack was propagated from a notched femur, there was a difference in crack initiation toughness ($K_{c,int}$) between the rat strains at 16-wks before hyperglycemia (Fig. 4c). Interestingly, $K_{c,int}$ and cracking toughness (Fig. 4d) did not vary with age for CD(SD) rats but decreased with duration of diabetes in the ZDSD rats such that the higher fracture toughness properties in ZDSD rats at 16-wks were no longer different between the groups at 29-wks.

3.9. Diabetes- and age-related changes in bone composition

With respect to the compositional properties of bone tissue (femur), the mineral-to-matrix ratio (MMR) was higher for ZDSD rats than for CD(SD) rats at all age groups for both calculations (υ_1PO_4/Amide I and υ_1PO_4/Proline), but these strain-related differences were only significant at 22-wks and 29-wks. Moreover, MMR increased with age, regardless of strain (Table 3). Interestingly, crystallinity did not vary with age in non-diabetic rats, but was higher after diabetic onset in the ZDSD rats. Although diabetes was a significant factor explaining the variance in pentosidine when accounting for age and body weight (Supplemental Table 1), there were no significant differences in PE between non-diabetic CD(SD) and diabetic ZDSD rats at each age (Fig. 5). The mature enzymatic collagen crosslinks (pyridinolines or PYD) increased with age in both strains.

4. Discussion

Skeletal fragility is now recognized a complication associated with T2D [35], but yet the underlying causes for the increased fracture risk among diabetics are currently not known. The present study supports, in part, the use of the ZDSD rat as a model of diabetic bone disease. Unlike the ZDF rat, ZDSD rats have normal leptin signaling and thus avoid the potential confounding effects of reduced leptin signaling in the hypothalamus on bone [36, 37]. Also, being a diet-induced model of T2D, overt hyperglycemia can be initiated after the animal reaches skeletal maturity within 2 weeks. Most importantly, cortical bone progressively lost toughness (radius) and fracture toughness (femur) with progression of diabetes. That is, diabetic ZDSD rats experience the hypothesized brittle effect that can also occur with advanced aging and possibly diabetes in humans. They also exhibit diabetes-related increase in cortical porosity, albeit the increase is small at 29-wks (Fig. 3). There are however a number of confounding issues with the ZDSD rat as follows: i) the ZDSD rats can also lose body weight as diabetes progresses, ii) there are structural differences in the diaphysis between ZDSD and control before the onset of hyperglycemia, iii) differences in material strength and fracture toughness between the rat strains exist before but not after diabetic onset, iv) trabecular bone volume fraction decreases with diabetes duration, which has not yet been observed in humans with T2D, and v) AGEs in bone are not different from control, though they appear to accumulate with diabetes duration.

One potential way to mitigate the weight loss in the ZDSD rat could involve stopping the HFD − used to time the onset of hyperglycemia − after 2 weeks. This assumes the high fat is driving the overt hyperglycemia and subsequent increase in glycosuria. However, when ZDSD male rats were solely fed Purina 5008 chow (16.7% kcal) in a different study, there was a similar weight gain through maturation, as in the present study, peaking around 23-wks (564.4 ± 8.2 g) and then subsequently significant weight loss over the next 8 weeks [27]. Of note, with Purina 5008 diet, the onset of overt diabetes in ZDSD rats was variable with the majority exceeding 250 mg/dl between 21-wks and 23-wks, instead of between 16-wks and 18-wks when consuming 5SCA. In another study in which 16-wk old CD(SD) male rats and ZDSD male rats were fed the 5SCA HFD between 16-wks and 22-wks, similar to the present study, the ZDSD rats (424 ± 15 g) weighed significantly less than the CD(SD) rats 527 ± 11 g) at 34-wks [38]. ZDSD rat is obviously not a model of obesity-associated diabetes.

Several previous studies have also documented differences in trabecular architecture and cortical structure between CD(SD) and ZDSD rats. In the first reported study in which male rats were fed Purina 5008 until death (33-wks), Reinwald et al ([23]) found that trabecular bone volume in the L4 VB was less for diabetic ZDSD than for non-diabetic CD(SD) strain as determined by μCT. Using HR-pQCT to assess the cortical structure of the femur diaphysis, cortical area and cortical thickness were all lower in the ZDSD rats. A conclusion to be drawn from the study is that diabetes worsens cortical bone structure, but strain-related differences in structure, namely moment of inertia, can exist prior to the ZDSD rats developing frank diabetes (Table 2). In the present study, BV/TV in the distal femur was not different between the rat strains at 16-wks but was lower for the ZDSD rats after 12–13 weeks of diabetes (Table 1). Moreover, in a previous study comparing non-diabetic ZDSD

rats to diabetic ZDSD rats (females fed 5SCA between 21-wks and 33-wks) [20], BV/TV in the distal femur was lower for the diabetic rats. To the best of our knowledge, the present study is the first to report that normal age-related changes in the cortical structure of the mid-shaft occurs in diabetic ZDSD male rats while a diabetes-related loss in trabecular bone also occurs. Also, the age-related increases in structure (I_{min}) and peak moment that occurred in both rat strains (Table 2) remained significant when accounting for the contribution of body weight (BW) to bone strength (Supplemental Table 1).

Several studies reported variable differences in the material properties between male CD(SD) and male ZDSD rats. In the initial report by Reinwald et al. [23], there were no significant differences in either peak bending strength or toughness (femur). Subsequently, Gallant et al. [39] reported lower bending strength and lower toughness of cortical bone for ZDSD rats compared to CD(SD) controls. Rats in the latter study were fed a HFD starting at 20 weeks for 12 weeks, suggesting that HFD may exacerbate the effects of diabetes on material properties of bone. However, in the aforementioned female ZDSD study [20], material properties were not significantly different. Presently, material strength, fracture toughness, and cracking toughness were higher for the ZDSD than for the male CD(SD) rats at 16-wks, but these material properties did not change or significantly decreased with diabetes duration in the ZDSD rat (Fig. 4). As a possible explanation for this lack of an age-related increase in material strength, circulating insulin decreases from normal levels with the progression of diabetes in ZDSD rats (Supplemental Fig. 1). Thus, the progression of diabetes in ZDSD male rats apparently affects the mechanical properties of the bone, in particular toughness and fracture toughness. However, the use of male CD(SD) rats as a control complicates this interpretation of diabetic effects on material properties as differences in the fracture properties and bending strength between the 2 rat groups are not significant at 29-wks. Differences in BW between CD(SD) and ZDSD rats do not explain the lack of an age-related increase in bending strength in ZDSD rats as body weight was not a significant explanatory variable of this material property (Supplemental Table 1).

NEG crosslinking in collagen (i.e., AGE accumulation) is thought to decrease the toughness of bone by preventing fibril sliding and energy dissipation of the tissue [19]. Saito et al [40] analyzed bones using the male WBN/Kob rat model of spontaneous T2D (no diet manipulation) in which male Wistar rats served as non-diabetic controls and reported that PE in the femoral cortex was higher for the T2D animals starting at 12 months (52-wks). The onset of overt diabetes in this study occurred between 10-mo. to 12-mo. with body weight significantly decreasing between 12-mo. and 14-mo in only WBN/Kob rats. As with this other rat model of T2D, we found that PE in the femoral cortex of ZDSD rat increased with duration of diabetes, but there was not a significant difference in PE between non-diabetic and diabetic bone. Possibly, to establish a difference in AGEs between non-diabetic and diabetic bone in ZDSD rats requires animals older than 29-wks, longer duration of diabetes than 12-wks, and/or non-obese animals as controls.

A previous study in which CD(SD) and ZDSD male rats were fed 5SCA for 2 weeks starting 17-wks [26] also found higher MMR in the long bones (tibia) from the diabetic than from the non-diabetic rats. Because we included 16-wk old rats, we were able to observe that diabetes does not impede age-related accumulation of mineral in the matrix. One

interpretation of the difference in MMR between non-diabetic and diabetic bone is that diabetes affects the amount of collagen. However, Raman is sensitive to the inherent polarization bias [41], so what could actually be different between CD(SD) and ZDSD rats is collagen fibril orientation.

The discrepancy in the duration-related decrease in bone toughness between the radius and femur is likely due to the limitations inherent in the mechanical testing of rodent long bones. Since machining uniform specimens from the cortex is exceedingly difficult and impractical, material properties like toughness are estimated from flexural tests of the diaphysis. Being more slender, the radius experiences less shear than does the femur and so its toughness is dictated more so by tensile behavior of the tissue. We cannot however rule out role of anatomical differences in how diabetes affects bone (e.g., differences in load bearing between the radius and femur). Nonetheless, the present study suggests that testing two different bones is useful in identifying how diabetes affects fracture resistance. The study also suggests that non-diabetic ZDSD rats would be a better a control than CD(SD) rats. Since female ZDSD rats are less susceptible to diabetes than male ZDSD rats fed a high fat diet, they would likely provide approximately equal numbers of non-diabetic and diabetic rats. The HFD also appears to help time the onset of diabetes (i.e., rats become hyperglycemic at the same age).

As diabetes progressed in the ZDSD rats, there were decreases in toughness and fracture toughness of cortical bone with no change in material strength, whereas bones from non-diabetic rats between 16-wks and 29-wks exhibited an increase in material strength of cortical bone but no changes in toughness and fracture toughness. While there are limitations to using the ZDSD rat as a model of diabetic bone disease, this model does implicate tissue-level properties as factors contributing to diabetic bone disease.

Supplementary Material

Refer to Web version on PubMed Central for supplementary material.

Acknowledgments

The Department of Veterans Affairs, Veterans Health Administration, Office of Research and Development (1I01BX001018) primarily funded the present work. The purchase of the micro-computed tomography scanner was supported by the National Center for Research Resources (1S10RR027631) and matching funds from the Vanderbilt Office of Research. There was additional support from the National Institute of Arthritis and Musculoskeletal and Skin Diseases of the National Institutes of Health (NIH grants AR063157 and 1T32DK101003) and the National Science Foundation (1068988). The Vanderbilt Hormone Assay and Analytical Services Core is supported by NIH grants DK059637 and DK020593. The content is solely the responsibility of the authors and does not necessarily represent the official views of the National Institutes of Health or other funding agencies.

Glossary

AGEs	Advanced glycation end products
α-ABA	Alpha-amino-N-butyric acid
aBMD	Areal bone mineral density

Ct.Ar	Bone cross-sectional area
BW	Body weight
BV/TV	Bone volume fraction
CD(SD)	CD IGS rat (Clr:CD(SD)) from Charles River
Conn.D	Connectivity density
Ct.Th	Cortical thickness
Ct.TMD	Cortical tissue mineral density
$K_{c,int}$	Crack initiation toughness
DPD	Deoxypyridinoline
DFM	Distal femur metaphysis
C_{min}	Distance between centroid and periosteal surface
EDTA	Ethylenediamine tetraacetic acid
HFBA	Heptafluorobutyric acid
HFD	High fat diet
HPLC	High performance liquid chromatography
HR-pQCT	High-resolution peripheral quantitative computed tomography
HA	Hydroxyapatite
Ct.Po	Intra-cortical porosity
μCT	Micro-computed tomography
MMR	Mineral-to-matrix ratio
I_{min}	Moment of inertia
NEGs	Non-enzymatic, glycation mediated crosslinks
M_p	Peak moment
PE	Pentosidine
PITC	Phenylisothiocyanate
PBS	Phosphate buffer saline
Po.N	Pore number
PY_{disp}	Post-yield displacement
PYD	Pyridinoline

PYR	Pyridoxine
RS	Raman spectroscopy
ROI	Region of interest
L	Span
3pt	Three-point bending
Tt.Ar	Total cross-sectional area
Tb.N	Trabecular number
Tb.Th	Trabecular thickness
Tb.TMD	Trabecular tissue mineral density
T2D	Type 2 diabetes
VB	Vertebrae
W_f	Work-to-fracture
ZDF	Zucker Diabetic Fatty
ZDSD	Zucker Diabetic Sprague Dawley from PreClinOmics

References

1. Bonds DE, Larson JC, Schwartz AV, Strotmeyer JR, Rodriguez BL, Johnson KC, Margolis KL. Risk of fracture in women with type 2 diabetes: the Women's Health Initiative Observational Study. J Clin Endocrinol Metab. 2006; 91:3404–3410. [PubMed: 16804043]
2. Vestergaard P, Rejnmark L, Mosekilde L. Diabetes and its complications and their relationship with risk of fractures in type 1 and 2 diabetes. Calcif Tissue Int. 2009; 84:45–55. [PubMed: 19067021]
3. Janghorbani M, Van Dam RM, Willett WC, Hu FB. Systematic review of type 1 and type 2 diabetes mellitus and risk of fracture. Am J Epidemiol. 2007; 166:495–505. [PubMed: 17575306]
4. Seeley DG. Predictors of ankle and foot fractures in older women. J Bone Miner Res. 1996; 11:1347. [PubMed: 8864910]
5. de Liefde II, van der Klift M, de Lae CE, van Daele PL, Hofman A, Pols HA. Bone mineral density and fracture risk in type-2 diabetes mellitus: the Rotterdam study. Osteoporos Int. 2005; 16:1713–1720. [PubMed: 15940395]
6. Leslie WD, Lix LM, Prior HJ, Derksen S, Metge C, O'Neil J. Biphasic fracture risk in diabetes: A population-based study. Bone. 2007; 40:1595–1601. [PubMed: 17392047]
7. Schwartz AV, Vittinghoff E, Bauer DC, Hillier TA, Strotmeyer ES, Ensrud KE, et al. Association of BMD and FRAX score with risk of fracture in older adults with type 2 diabetes. JAMA. 2011; 305:2184–2192. [PubMed: 21632482]
8. Burghardt A, Issever AS, Schwartz AV, Davis KA, Masharani U, Majumdar S, et al. High-resolution peripheral quantitative computed tomographic imaging of cortical and trabecular bone microarchitecture in patients with type 2 diabetes mellitus. J Clin Endocrinol Metab. 2010; 95:5045–5055. [PubMed: 20719835]
9. Farr JN, Drake MT, Amin S, Melotn LJ 3rd, McCready LK, Khosla S. In Vivo assessment of bone quality in postmenopausal women with type 2 diabetes. J Bone Miner Res. 2014; 29:787–795. [PubMed: 24123088]

10. Yu E, Putman MS, Derrico N, Abrishamanian-Garcia G, Finkelstein JS, Bouxsein ML. Defects in cortical microarchitecture among African-American women with type 2 diabetes. Osteoporos Int. 2015; 26:673–679. [PubMed: 25398431]
11. Patsch JM, Burghardt AJ, Yap SP, Baum T, Schwartz AV, Joseph GB, Link TM. Increased cortical porosity in type 2 diabetic postmenopausal women with fragility fractures. J Bone Miner Res. 2013; 28:313–324. [PubMed: 22991256]
12. Heilmeier U, Carpenter DR, Patsch JM, Harnish R, Joseph GB, Burghardt AJ, Baum T, Schwartz AV, Lang TF, Link TM. Volumetric femoral BMD, bone geometry, and serum sclerostin levels differ between type 2 diabetic postmenopausal women with and without fragility fractures. Osteoporos Int. 2015; 26:1283–1293. [PubMed: 25582311]
13. Vestergaard P. Discrepancies in bone mineral density and fracture risk in patients with type 1 and type 2 diabetes - a meta-analysis. Osteoporos Int. 2006; 18:427–444. [PubMed: 17068657]
14. Nyman JS, Roy A, Tyler JH, Acuna RL, Gayle HJ, Wang X. Age-related factors affecting the postyield energy dissipation of human cortical bone. J Orthop Res. 2007; 25:646–655. [PubMed: 17266142]
15. Karim L, Tang SY, Sroga GE, Vashishth D. Differences in non-enzymatic glycation and collagen cross-links between human cortical and cancellous bone. Osteoporos Int. 2013; 24:2441–2447. [PubMed: 23471564]
16. Zimmermann EA, Schaible E, Bale H, Barth HD, Tang SY, Reichert P, Busse B, Alliston T, Ager JW 3rd, Ritchie RO. Age-related changes in the plasticity and toughness of human cortical bone at multiple length scales. Proc Natl Acad Sci USA. 2011; 108:14416–144421. [PubMed: 21873221]
17. Monnier V, Sun W, Sell DR, Fan X, Nemet I, Genuth S. Glucosepane: a poorly understood advanced glycation end product of growing importance for diabetes and its complications. Clin Chem Lab Med. 2014; 52:21–32. [PubMed: 23787467]
18. Oren TW, Botolin S, Williams A, Buckness A, King KB. Arthroplasty in veterans: Analysis of cartilage, bone, serum, and synovial fluid reveals differences and similarities in osteoarthritis with and without comorbid diabetes. J Rehabil Res Dev. 2011; 48:1195–1210. [PubMed: 22234664]
19. Saito M, Kida Y, Kato S, Marumo K. Diabetes, collagen and bone quality. Curr Osteoporos Rep. 2014; 12:181–188. [PubMed: 24623537]
20. Hill Gallant KM, Gallant MA, Brown DM, Sato AY, Williams JN, Burr DB. Raloxifene prevents skeletal fragility in adult female Zucker Diabetic Sprague-Dawley rats. PLoS One. 2014; 9:e108262. [PubMed: 25243714]
21. Prisby RD, Swift JM, Bloomfield SA, Hogan HA, Delp MD. Altered bone mass, geometry, and mechanical properties during the development and progression of type 2 diabetes in the Zucker diabetic fatty rat. J Endocrinol. 2008; 199:379–388. [PubMed: 18755885]
22. Hamann C, Picke AK, Campbell GM, Balyura M, Rauner M, Bernhardt R, Huber G, Morlock MM, Günther KP, Borstein Stefan R, Gluer Claus-C, Ludwig Barbara, Hofbauer Lorenz C. Effects of parathyroid hormone on bone mass, bone strength, and bone regeneration in male rats with type 2 diabetes mellitus. Endocrinology. 2014; 155:1197. [PubMed: 24467747]
23. Reinwald S, Peterson RG, Allen MR, Burr DB. Skeletal changes associated with the onset of type 2 diabetes in the ZDF and ZDSD rodent models. Am J Physiol Endocrinol Metab. 2009; 296:E765–E774. [PubMed: 19158319]
24. Nyman JS. Effect of diabetes on the fracture resistance of bone. Clinic Rev Bone Miner Metab. 2013; 11:38–48.
25. Fajardo RJ, Karim L, Calley VI, Bouxsein ML. A review of rodent models of type 2 diabetic skeletal fragility. J Bone Miner Res. 2014; 29:1025–1040. [PubMed: 24585709]
26. Hammond MA, Gallant MA, Burr DB, Wallace JM. Nanoscale Changes in collagen are reflected in physical and mechanical properties of bone at the microscale in diabetic rats. Bone. 2014; 60:26–32. [PubMed: 24269519]
27. Peterson RG, Jackson CV, Zimmerman K, de Winter W, Hueber N, Hansen MK. Characterization of the ZDSD rat: A translational model for the study of the metabolic syndrome and type 2 diabetes. J Diabetes Res. 2015:487816. [PubMed: 25961053]

28. Bouxsein ML, Boyd SK, Christiansen BA, Guldberg RE, Jepsen KJ, Müller R. Guidelines for assessment of bone microstructure in rodents using micro-computed tomography. J Bone Miner Res. 2010; 25:1468–1486. [PubMed: 20533309]
29. Uppuganti S, Granke M, Makowski AJ, Does MD, Nyman JS. Age-related changes in the fracture resistance of male Fischer F344 rat. Bone. 2016; 83:220–232. [PubMed: 26610688]
30. Silva MJ, Brodt MD, Lynch MA, McKenzie JA, Tanouye KM, Nyman JS, Wang X. Type 1 diabetes in young rats leads to progressive trabecular bone loss, cessation of cortical bone growth, and diminished whole bone strength and fatigue life. J Bone Miner Res. 2009; 24:1618–1627. [PubMed: 19338453]
31. Ritchie R, Koester KJ, Ionova S, Yao W, Lane NE, Ager JW. Measurement of the toughness of bone: A tutorial with special reference to small animals. Bone. 2008; 43:798–812. [PubMed: 18647665]
32. Makowski AJ, Uppuganti S, Wadeer SA, Whitehead JM, Rowland BJ, Granke M, Mahadevan-Jansen A, Yang X, Nyman JS. The loss of activating transcription factor 4 (ATF4) reduces bone toughness and fracture toughness. Bone. 2014; 62:1–9. [PubMed: 24509412]
33. Makowski AJ, Pence IJ, Uppuganti S, Zein-Sabatto A, Huszagh MC, Mahadevan-Jansen A, Nyman JS. Polarization in Raman spectroscopy helps explain bone brittleness in genetic mouse models. J Biomed Opt. 2014; 19:117008. [PubMed: 25402627]
34. Buckley, A.; Hill, KE.; Davidson, JS. Collagen metabolism. In: Di Sabato, G.; Abelson, J.; Simon, M., editors. Methods in Enzymology. San Diego: Academic Press; 1988. p. 674-694.
35. Shanbhogue V, Michell DM, Rosen CJ, Bouxsein ML. Type 2 diabetes and the skeleton: new insights into sweet bones. Lancet Diabetes Endocrinology. 2015; 4:159–173. [PubMed: 26365605]
36. Takeda S, Elefteriou F, Levasseur R, Liu X, Zhao L, Parker KL, Armstrong D, Ducy P, Karsenty G. Leptin regulates bone formation via the sympathetic nervous system. Cell. 2002; 111:305–317. [PubMed: 12419242]
37. Shi Y, Yadav VK, Suda N, Liu XS, Guo XE, Myers MG, Karsenty G. Dissociation of the neuronal regulation of bone mass and energy metabolism by leptin in vivo. Proc Natl Acad Sci USA. 2008; 105:20529–20533. [PubMed: 19074282]
38. Davidson E, Coppey LJ, Holmes A, Lupachy S, Dake BL, Oltman CL, Peterson RG, Yorek MA. Characterization of diabetic neuropathy in the Zucker Diabetic Sprague-Dawley Rat: A new animal model for type 2 diabetes. J Diabetes Res. 2014:714273. [PubMed: 25371906]
39. Gallant MA, Brown DM, Organ JM, Allen MR, Burr DB. Reference-Point Indentation correlates with bone toughness assessed using whole-bone traditional mechanical testing. Bone. 2013; 53:301–305. [PubMed: 23274349]
40. Saito M, Fujii K, Mori Y, Marumo K. Role of collagen enzymatic and glycation induced cross-links as a determinant of bone quality in spontaneously diabetic WBN/Kob rats. Osteoporos Int. 2006; 17:1514–1523. [PubMed: 16770520]
41. Makowski A, Patil CA, Mahadevan-Jansen A, Nyman JS. Polarization control of Raman spectroscopy optimizes the assessment of bone tissue. J Biomed Opt. 2013; 18:55005. [PubMed: 23708192]

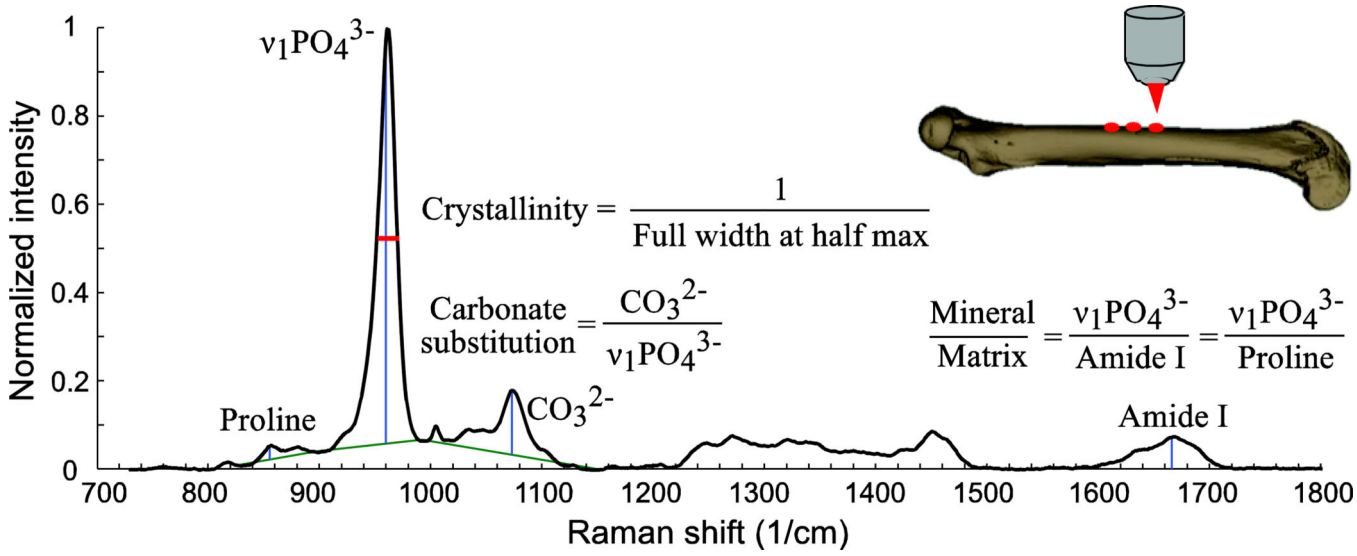

Figure 1.

Raman spectrum of bone as collected from the femur mid-shaft with calculation of compositional properties. Calculating peak ratios and the width of the most prominent peak provided compositional properties of bone tissue.

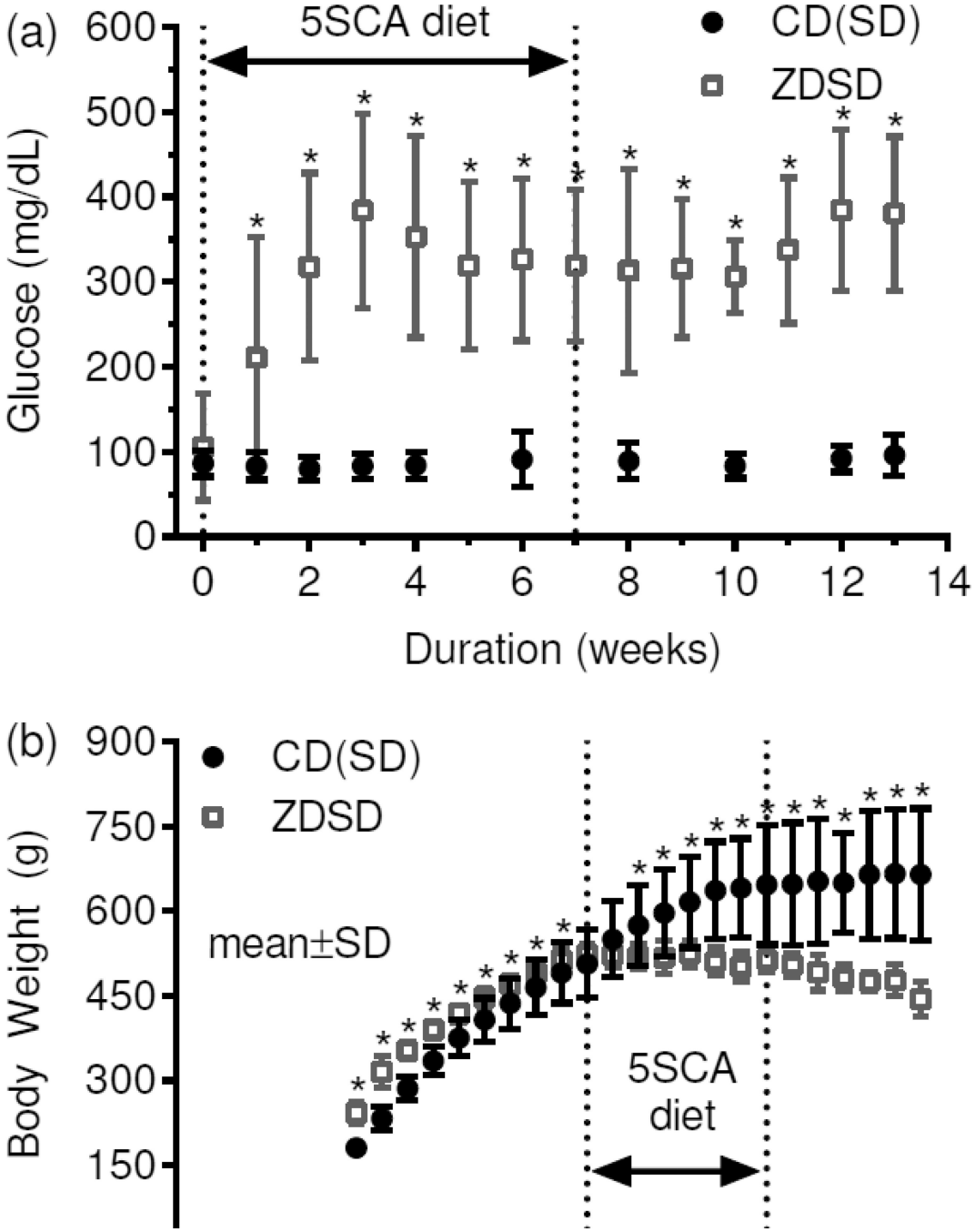

Figure 2.

Non-fasting glucose levels over time after switching to a high fat diet (a) and body weight vs. age (b). ZDSD rats had significantly higher glucose levels than CD(SD) rats by 17-wks. CD(SD) rats became obese on the HFD but ZDSD rats began to lose weight. * indicates significant difference between ZDSD values and CD(SD).

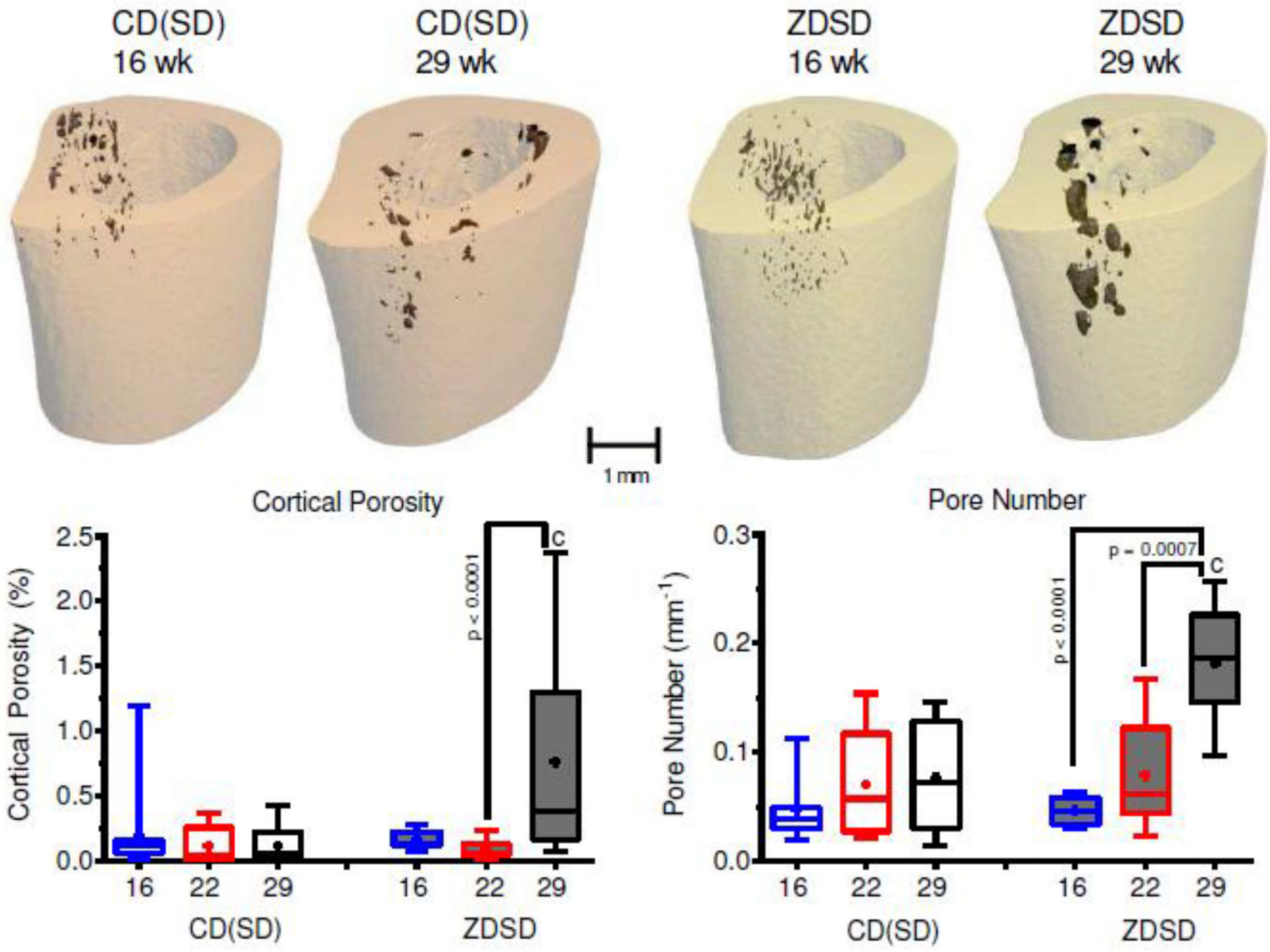

Figure 3.

μCT analysis of porosity in cortical bone within the femoral mid-shaft of ZDSD and CD(SD) rats. Cortical porosity and pore number was higher for ZDSD than for CD(SD) rats at 29-wks. [c]p=0.0006 for CD(SD) vs. ZDSD at 29-wks.

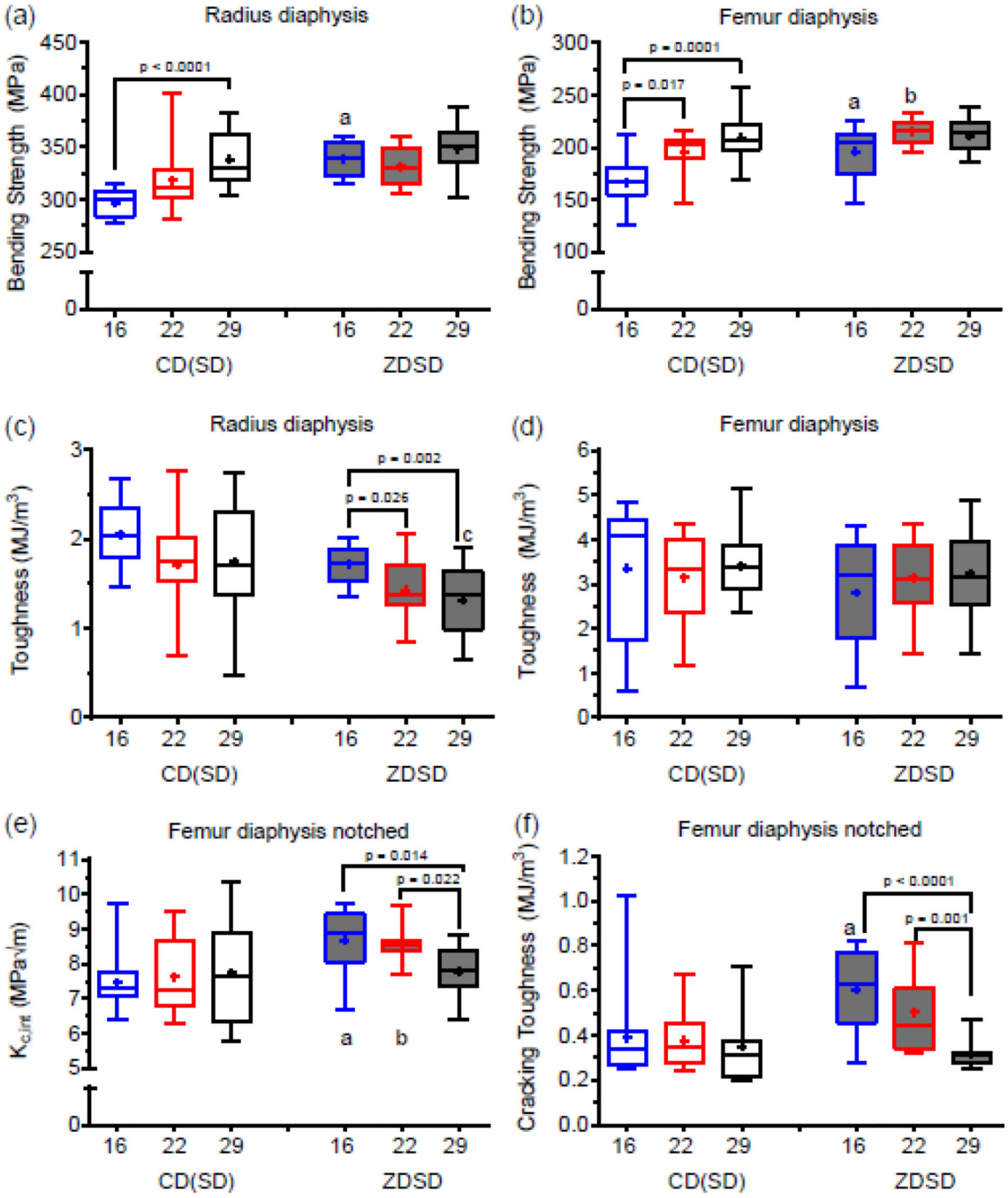

Figure 4.

Selected apparent-level material properties as determined by flexural tests of long bones. With aging, estimated material strength of the radius (a) and femur (b) increased for the CD(SD) rats but did not change for the ZDSD rats. As the duration of T2D increased, toughness decreased for the ZDSD rats (c: radius only), but toughness did not vary with age for the non-diabetic rats (c, d). Resistance to crack initiation (e) and energy to propagate a crack to failure (f) also decreased with increasing duration of diabetes in ZDSD rats. [a]$p<0.05$, [b]$p<0.05$, [c]$p<0.05$ for CD(SD) vs. ZDSD at 16-, 22-, and 29-wks, respectively.

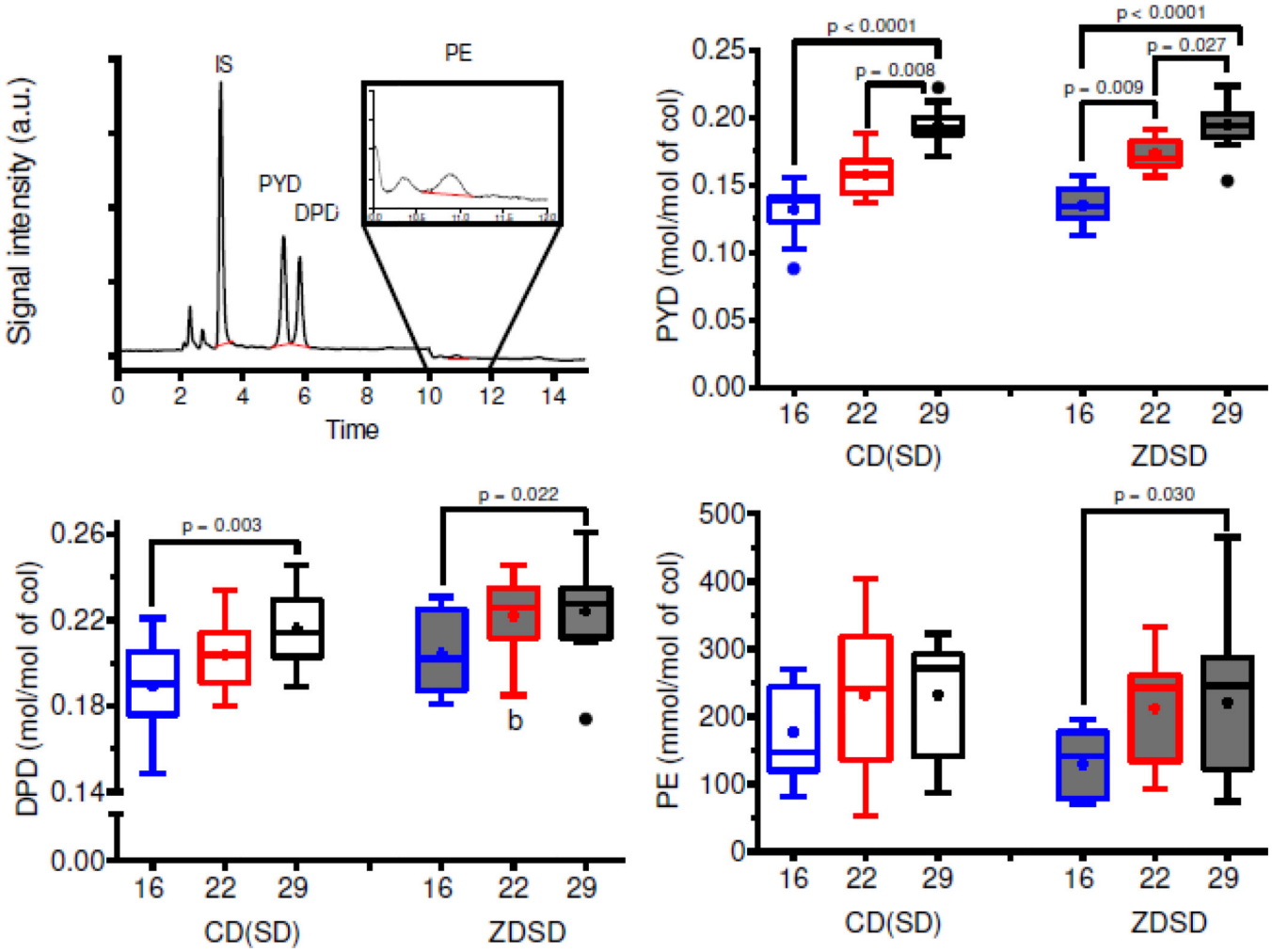

Figure 5.

Enzymatic and non-enzymatic crosslink concentration differences with a typical chromatogram for the elution of crosslinks shown in top left panel. Pentosidine increased with age or duration of diabetes in the ZDSD rat bone, but not vary with aging in the CD(SD) rat bone. [b]p=0.002 indicate for CD(SD) vs. ZDSD at 22-wks.

Table 1

Selected architectural properties of trabecular bone (mean±SD) as determined from μCT analysis of the distal femur metaphysis and lumbar vertebra of non-diabetic CD(SD) rats and ZDSD rats at different ages (and durations of hyperglycemia).

		16-wks of age (baseline data)			22-wks of age (5–6 weeks)			29-wks of age (12–13 weeks)		
Property	**Unit**	**CD(SD)**	**ZDSD**	**p-value**	**CD(SD)**	**ZDSD**	**p-value**	**CD(SD)**	**ZDSD**	**p-value**
Femur Metaphysis										
BV/TV	%	19.5 ± 3.9	20.1 ± 2.8	> 0.99	20.6 ± 4.8	18.2 ± 1.7	0.611	20.3 ± 5.1	12.6 ± 1.8 *#	**< 0.0001**
Tb.Th	mm	0.089 ± 0.008	0.089 ± 0.004	> 0.99	0.093 ± 0.008	0.086 ± 0.004	0.232	0.098 ± 0.011	0.072 ± 0.005 *#	**< 0.0001**
Tb.N	1/mm	2.49 ± 0.49	2.44 ± 0.32	> 0.99	2.46 ± 0.78	2.27 ± 0.29	> 0.99	2.30 ± 0.54	2.14 ± 0.26 *	> 0.99
Conn.D	$1/mm^3$	71.9 ± 13.3	64.7 ± 5.6	> 0.99	65.3 ± 16.5	62.1 ± 6.6	> 0.99	51.4 ± 14.1 *	50.5 ± 8.4 *#	> 0.99
Tb.TMD	$mgHA/cm^3$	948 ± 13	950 ± 8	> 0.99	967 ± 16	978 ± 9 *	0.321	1000 ± 16 *#	977 ± 9 *	0.067
L6 vertebra										
BV/TV	%	35.9 ± 3.4	34.0 ± 2.2	> 0.99	39.9 ± 5.9	34.1 ± 2.7	0.157	37.4 ± 4.0	25.9 ± 2.5 *#	**< 0.0001**
Tb.Th	mm	0.088 ± 0.006	0.086 ± 0.005	> 0.99	0.099 ± 0.011 *	0.091 ± 0.007	0.594	0.097 ± 0.008 *	0.075 ± 0.005 *#	**< 0.0001**
Tb.N	1/mm	4.17 ± 0.26	4.20 ± 0.14	> 0.99	4.18 ± 0.40	4.02 ± 0.13	0.603	4.09 ± 0.44	3.84 ± 0.17 *	**0.021**
Conn.D	$1/mm^3$	109.7 ± 13.3	101.5 ± 6.7	0.695	94.9 ± 15.5	93.0 ± 7.3	> 0.99	94.1 ± 24.2 *	103.1 ± 9.3 #	0.057
Tb.TMD	$mgHA/cm^3$	977 ± 8	969 ± 12	0.951	999 ± 16 *	995 ± 11 *	> 0.99	1010 ± 18 *	988 ± 11 *	**0.005**

*Significantly different from 16 week age group (baseline) and

#significantly different from 22 week age group as determined by Dunn's test within rat strain. Otherwise, p-values are given for CD(SD) vs. ZDSD within each age (Dunn's test).

Calcif Tissue Int. Author manuscript; available in PMC 2017 September 01.

Table 2

Selected properties of cortical bone (mean±SD) as determined from the analyses of long-bones of non-diabetic CD(SD) rats and ZDSD rats at different ages (and durations of hyperglycemia).

		16-wks of age (baseline)			22-wks of age (5–6 weeks)			29-wks of age (12–13 weeks)		
Property	**Unit**	**CD(SD)**	**ZDSD**	**p-value**	**CD(SD)**	**ZDSD**	**p-value**	**CD(SD)**	**ZDSD**	**p-value**
Femur mid-shaft										
Length[a]	mm	36.5 ± 0.9	34.3 ± 0.9	**0.011**	38.4 ± 1.0 *	36.2 ± 0.6 *	**0.0002**	38.9 ± 1.1 *	36.8 ± 0.5 *	**0.002**
Ct.Th[b]	mm	0.701 ± 0.027	0.734 ± 0.024	> 0.99	0.902 ± 0.055 *	0.868 ± 0.026 *	> 0.99	0.924 ± 0.058 *	0.826 ± 0.025 *#	**0.002**
Ct.Ar[b]	mm^2	7.44 ± 0.47	6.97 ± 0.48	0.963	9.33 ± 1.04 *	8.33 ± 0.40 *	0.154	9.83 ± 1.04 *	8.28 ± 0.33 *	**0.006**
Tt.Ar[b]	mm^2	7.46 ± 0.48	6.99 ± 0.48	0.985	9.34 ± 1.05 *	8.34 ± 0.40 *	0.152	9.85 ± 1.05 *	8.34 ± 0.36 *	**0.009**
I_{min}[b]	mm^4	8.29 ± 1.37	6.32 ± 0.82	**0.009**	10.46 ± 2.15 *	8.11 ± 0.90 *	**0.016**	11.41 ± 2.43 *	8.49 ± 0.90 *	**0.013**
Ps.Pm	mm	13.9 ± 0.7	12.8 ± 0.5	**0.001**	14.7 ± 0.8	13.7 ± 0.3 *	**0.015**	14.9 ± 0.8 *	13.8 ± 0.4 *	**0.010**
Ct.TMD[b]	$mgHA/cm^3$	1214 ± 9	1211 ± 7	> 0.99	1241 ± 12 *	1239 ± 6 *	> 0.99	1269 ± 13 *#	1267 ± 7 *#	> 0.99
Rigidity[c]	GPa	39.9 ± 4.3	36.3 ± 4.1	> 0.99	65.8 ± 13.3 *	50.4 ± 6.6 *	**0.039**	73.4 ± 18.4 *	56.3 ± 6.2 *	0.201
Modulus[c]	GPa	4.86 ± 0.72	5.77 ± 0.67	0.187	6.27 ± 0.44 *	6.23 ± 0.85	> 0.99	6.42 ± 0.90 *	6.62 ± 0.57 *	> 0.99
M_p[c]	N·mm	771 ± 110	732 ± 105	> 0.99	1072 ± 188 *	979 ± 84 *	> 0.99	1244 ± 241 *	991 ± 70 *	**0.047**
PY_{disp}[c]	1/mm	0.024 ± 0.015	0.017 ± 0.011	0.212	0.020 ± 0.008	0.018 ± 0.008	> 0.99	0.022 ± 0.006	0.022 ± 0.010	> 0.99
W_f[c]	N·mm	132 ± 56	100 ± 46	0.177	164 ± 45	140 ± 37	0.400	191 ± 42 *	147 ± 39 *	0.065
Radius										
Length[a]	mm	27.5 ± 0.9	25.8 ± 0.6	**0.007**	29.0 ± 0.6 *	26.7 ± 1.1	**<0.0001**	29.4 ± 0.9 *	27.5 ± 0.3 *	**0.0002**
Ct.Th[b]	mm	0.489 ± 0.033	0.512 ± 0.021	> 0.99	0.582 ± 0.034 *	0.566 ± 0.035 *	> 0.99	0.651 ± 0.056 *	0.610 ± 0.023 *#	0.590
Ct.Ar[b]	mm^2	2.30 ± 0.20	1.89 ± 0.14	**0.0002**	2.64 ± 0.33 *	2.16 ± 0.11 *	**0.001**	2.77 ± 0.39 *	2.22 ± 0.12 *	**0.001**
Tt.Ar[b]	mm^2	2.45 ± 0.23	2.04 ± 0.15	**0.0002**	2.75 ± 0.37	2.36 ± 0.42 *	**0.008**	2.86 ± 0.41 *	2.29 ± 0.11 *	**0.0006**
Ps.Pm	mm	6.33 ± 0.32	5.71 ± 0.30	**<0.0001**	6.58 ± 0.42	6.08 ± 0.18 *	**0.007**	6.60 ± 0.53	6.16 ± 0.20 *	**0.040**
I_{min}[b]	mm^4	0.442 ± 0.062	0.287 ± 0.044	**<0.0001**	0.533 ± 0.126	0.380 ± 0.056 *	**0.003**	0.589 ± 0.165 *	0.401 ± 0.053 *	**0.002**
Ct.TMD[b]	$mgHA/cm^3$	1131 ± 11	1140 ± 6	> 0.99	1162 ± 18 *	1154 ± 19	> 0.99	1192 ± 14 *#	1180 ± 10 *#	0.692
Rigidity[c]	GPa	2.31 ± 0.35	1.84 ± 0.21	**0.009**	2.86 ± 0.42 *	2.13 ± 0.15 *	**0.0004**	3.32 ± 0.61 *	2.39 ± 0.22 *#	**0.004**

		16-wks of age (baseline)			22-wks of age (5–6 weeks)			29-wks of age (12–13 weeks)		
Property	**Unit**	**CD(SD)**	**ZDSD**	**p-value**	**CD(SD)**	**ZDSD**	**p-value**	**CD(SD)**	**ZDSD**	**p-value**
M_p[c]	N·mm	149 ± 22	121 ± 15	**0.019**	186 ± 28[*]	144 ± 11[*]	**0.004**	214 ± 43[*]	159 ± 15[*]	**0.014**
PY_{disp}[c]	1/mm	0.034 ± 0.006	0.028 ± 0.003	0.781	0.026 ± 0.008	0.022 ± 0.005[*]	0.419	0.025 ± 0.010[*]	0.019 ± 0.005[*]	0.126
W_f[c]	N·mm	32.0 ± 5.6	23.1 ± 3.1	**0.002**	31.2 ± 6.5	22.1 ± 3.1	**0.0008**	33.6 ± 6.2	22.2 ± 4.1	< **0.0001**

[a] Caliper measurement of femur;

[b] μCT-derived measurement; and

[c] Biomechanical measurements as determined by three-point bending

[*] Significantly different from 16 week age group (baseline) and

[#] significantly different from 22 week age group as determined by Dunn's test within rat strain. Otherwise, p-values are given for CD(SD) vs. ZDSD within each age (Dunn's test).

Table 3

Selected compositional properties of cortical bone (mean±SD) as determined from Raman spectroscopy analysis of the femur mid-shaft.

Property	Unit	16-wks of age (baseline data)			22-wks of age (5–6 weeks)			29-wks of age (12–13 weeks)		
		CD(SD)	ZDSD	p-value	CD(SD)	ZDSD	p-value	CD(SD)	ZDSD	p-value
Femur										
υ_1PO_4/AmI[a]		9.88 ± 1.68	11.37 ± 1.83	0.774	12.07 ± 1.80 *	14.66 ± 0.70 *	**0.003**	12.87 ± 1.49 *	15.12 ± 0.90 *	**0.001**
υ_1PO_4/Pro		18.0 ± 3.5	22.3 ± 4.9	0.305	21.7 ± 4.0	29.6 ± 2.5 *	**0.0006**	24.8 ± 3.4 *	31.0 ± 2.3 *	**0.001**
Carb/Phosv1		0.146 ± 0.009	0.153 ± 0.007	0.368	0.152 ± 0.009	0.153 ± 0.006	> 0.99	0.166 ± 0.008 *#	0.170 ± 0.006 *#	0.916
$[FWHM]^{-1}$		0.061 ± 0.004	0.061 ± 0.003	> 0.99	0.061 ± 0.003	0.069 ± 0.003 *	**<0.0001**	0.061 ± 0.003	0.068 ± 0.004 *	**0.0001**

*Significantly different from 16 week age group (baseline) and

#significantly different from 22 week age group as determined by Dunn's test within rat strain. Otherwise, p-values are given for CD(SD) vs. ZDSD within each age (Dunn's test).

[a]The mineral-to-matrix ration (MMR) was determined by two ratios: the prominent phosphate peak normalized to either the Amide I peak or the proline peak (Fig. 1).